EPJ Web of Conferences **308**, 01006 (2024) https://doi.org/10.1051/epjconf/202430801006
ISRD 17

On the effect of the core boundary power distribution on the radiation situation in reactor components

Michal Košťál[1,*], *Vít* Klupák[1], *Zdeněk* Matěj[2], *Filip* Mravec[2], *František* Cvachovec[3], *Vojtěch* Rypar[1], *Evžen* Losa[1], *David* Harut[1], *Martin* Schulc[1], *Bohumil* Jánský[1], *Evžen* Novák[1], *Tomáš* Czakoj[1], *Alena* Krechlerova[1], *Vlastimil* Juříček[1], and *Sergey* Zaritskyi[4]

[1]Research Center Rez, Husinec-Rez, 250 68, 130, Czech Republic
[2]Masaryk University, Botanická 15, Brno 612 00, Czech Republic
[3]University of Defence, Kounicova 65, 662 10 Brno, Czech Republic
[4]NRC Kurchatov Institute Sciences, Russia

Abstract. The assessment of the neutron flux distribution in nuclear power plant components, like reactor internals and the pressure vessel, is one of the most important parts of their residual lifetime evaluation process because the irradiation damage of these components is strongly dependent on it. The fast neutron fluences in power reactors are generally determined using calculations and verified by measurements. Discrepancies between them sometimes occur, which can be caused by be the inaccuracies in the power distribution used in neutron transport calculations. This paper quantifies the effect of uncertainty in power density on the neutron fluences behind the reactor pressure vessel (RPV). An increase in power density was experimentally simulated by implementing a higher uranium enrichment of certain selected pins. The experiment was also simulated using the MCNP code with the ENDF/B-VII.1 library. Both the experimental and calculational data show a significant local increase in neutron flux. Even behind the RPV, the increase is as high as 25%, while the local power increase in the perturbed pins is about 70–80%, which is approximately equal to the 2σ power density uncertainties. A good agreement between measurement and calculation was found.

1 Introduction

The essentials of in-service programs for a realistic and reliable assessment of the reactor pressure vessel residual lifetime consist of a surveillance specimens' program [1] combined with the neutron fluences evaluation [2]. The neutron fluence in reactor components is determined by means of calculations fitted by experimental data [3]. The reliability of such an approach is determined through deviations between the calculated and experimental data. The deviation limits are described in methodologies of neutron flux determination such as

* Corresponding author: Michal.Kostal@cvrez.cz

the NRC Guide [4] and the NTD A.S.I. [5], and in case of a deviation of more than 30% behind the reactor pressure vessel (RPV) , the differences should be explained.

There might be more reasons for discrepancies. For example, every calculation is sensitive to the precision of the transport cross sections being used. Therefore, many experiments focused on the validation of important structural material cross sections were performed [6]. Another reason for possibly discrepant calculations is using an incorrect neutron source in transport calculations. In reactor dosimetry, the neutron source is mostly determined using a diffusion approach. This is a traditional technique, but sometimes there might be problems in the boundary regions [7]. Another issue might be incorrectness due to improper determination of burnup [8].

Another question is how the local power increase in the boundary core position is reflected in the neutron flux behind the RPV. To answer the questions above, a set of experiments was realised in a VVER-1000 Mock-Up placed in a zero power reactor LR-0 [9]. Its nuclear fuel is dismountable, and practically any arbitrary geometry can be simulated when limits and conditions of safety operation are fulfilled. In this experiment, the local power increase was simulated by replacing the original Mock-Up fuel pins by slightly more enriched pins. The shift in neutron flux profile was observed in both the reactor internals' simulator and the VVER-1000 RPV simulator [10, 11].

2 The Reactor Arrangements

The experiments were carried out in the VVER-1000 Mock-Up, which is a full-scale simulator of the VVER-1000 reactor in a radial sense forming ~ 120 degrees segment of the VVER-1000 core including the reactor baffle and barrel models. Except shortening of the fissile column to 125 cm, the simulator uses identical components in the radial direction. The Mock-Up is operated at atmospheric pressure and room temperature. To compensate for the lower density of the water in the VVER reactor in the direction out of the core, an air displacer is used in the VVER-1000 Mock-Up.

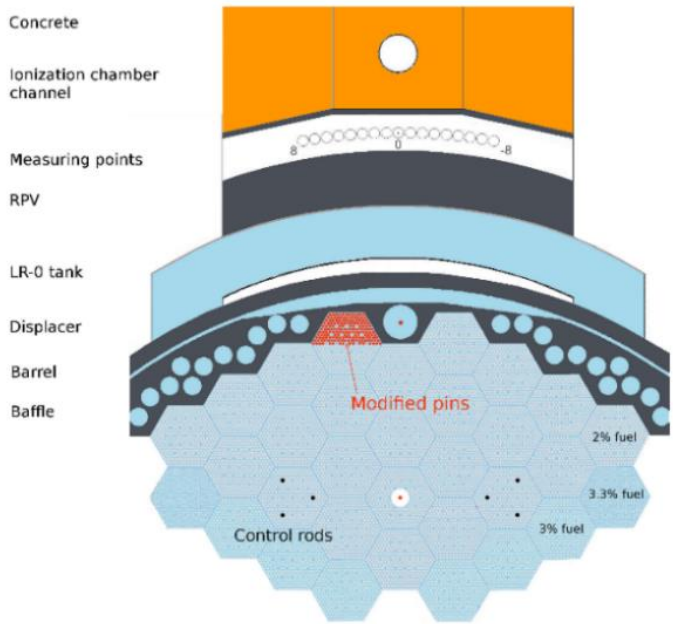

Fig. 1. Scheme of Mock-Up with marked measuring positions behind RPV simulator [10].

Due to this resemblance, the experiment realised in this core can be used for validation of the methods, models, and codes used for VVER reactor dosimetry issues. The standard Mock-Up core consists of 32 fuel assemblies with different ^{235}U enrichment levels, namely 24 × 2%, 6 × 3% and 2 × 3.3%. In the experiment, a modified core was assembled as well, where pins with 3.6% enrichment were inserted into a boundary assembly composed of 2% pins. The scheme of the Mock-Up core with marked measurement positions behind the RPV simulator, as well as in core measuring positions, is given in Fig. 1.

3 Experimental and Calculation Methods

The spatial distribution of the neutron flux was measured using an organic crystal scintillation spectrometer covering the energy interval 0.9 – 10 MeV. The power density was characterised by gamma spectrometry of fission products in the selected irradiated fuel pins. The neutron flux in the reactor internals was characterised using activation detectors.

3.1 Stilbene measurement

The measurements were realised behind the RPV in a VVER-1000 transport Mock-Up. The neutron spectra in the 0.9 to 10 MeV energy range were measured via the proton-recoil method using a stilbene scintillator (10 mm × 10 mm) with neutron and gamma pulse shape discrimination (hereinafter stilbene). The results of measurements are group fluxes with neutron energy above 1 MeV, which are compared to each other to investigate the flux azimuthal profile in the region behind the RPV.
A Pulse Shape Discrimination (PSD) unit is used to distinguish the type of the detected particle by analysing the pulse shape. The PSD value (D) is computed inside the field programmable gate array (FPGA) by an integration method which uses the comparison of the area delimited by a part of a trailing edge of the measured response (Q1) with the area delimited by the whole response (Q2). The Q1 and Q2 areas, expressed as the integrals over time, are shown in (Equation 1). More details can be found in [10].

$$Q_1 = \int_{t_1}^{t_2} i(t)dt, \quad Q_2 = \int_{t_0}^{t_2} i(t)dt, \quad D = \frac{Q_1}{Q_2} \tag{1}$$

3.2 Fission density measurement

The fission density was derived from the measured activity of the fission product ^{92}Sr (see Equations 2 - 4), which was induced during a 2.5-hour irradiation. Different power levels in different irradiation experiments were used depending on the position of the pins being measured (to obtain a reasonable measurement time). The net peak areas (NPAs) were measured using a collimated HPGe detector. Due to good knowledge of both the collimator and the HPGe detector, the measurement efficiencies could be determined by calculation. It was proven that the uncertainty in the calculated efficiency is not higher than 1.9% [9]. The reactor core layout with marked measured fuel assemblies and fuel pins is shown in Fig. 1.
The obtained fission densities were scaled to the same power level using activation foils (Au, Ni), monitoring absolute power in each experiment. These foils were irradiated during fuel activation. NPAs of these reactions were measured using another HPGe detector. The efficiency in the foil measurement was also determined by calculation using a validated mathematical model of the HPGe detector. Likewise, the uncertainties related with this

approach are not higher than 1.9%. More details can be found in [11]. Hereunder, the expressions for the fission density and accompanying variables are given:

$$F^j = \frac{A^j_{End}}{\lambda} \times \frac{1}{N^j_{End}} \quad (2)$$

$$A_{\mathrm{End}} = NPA(T_{\mathrm{Meas.}}) \times \frac{\lambda}{\varepsilon \times \eta} \times \frac{1}{\left(1-e^{-\lambda.T_{\mathrm{Meas.}}}\right)} \times \frac{1}{e^{-\lambda.\Delta T}} \times \frac{1}{k_{\mathrm{CSCF}}} \quad (3)$$

$$q\left(\overline{P}\right) = A_{\mathrm{End}}/N \times \left(1 - e^{-\lambda.T_{\mathrm{Irr}}}\right)^{-1} \quad (4)$$

where F^j is the fission rate determined via the i-th nuclide and j-th pin; N^j_{End} is the calculated number of observed nuclei in the j-th fuel pin at the end of the irradiation when 1 fission/s occurs; $NPA(T_{\mathrm{Meas.}})$ is the measured Net Peak Area of the observed nuclei i and corresponding selected peak; $T_{\mathrm{Meas.}}$ is the beginning of the measurement interval; λ is the decay constant of selected nuclide; η is the efficiency of the HPGe detector for the selected gamma line; ε is the gamma branching ratio of the selected peak; k_{CSCF} is the coincidence summing correction factor; ΔT is the length of the j-th pin HPGe measurement; $q\left(\overline{P}\right)$ is the reaction rate for the average power $\overline{P}$ and N is number of nuclei in the activation foil.

3.3 Calculation methods

Calculations were performed using the MCNP6 Monte Carlo code [12] and the ENDF/B-VII.1 [13] data library. The neutron fluxes behind the RPV were calculated using a fixed source model, as it makes calculation much more efficient. The neutron source for the fixed source model, in the form of neutron emission density, was calculated with a critical model. The calculated k_{eff} (1.005) was obtained in both the critical models, where the first was the standard mock up case and the second was the case with 164 replaced pins.
The source term used in the fixed source approach could be defined via the fission density thanks to the proportionality between the neutron emission density and the fission density. This proportionality reflects nearly identical neutron yield per fission in various pins. The pin power density distribution in the core was determined in a critical calculation. To obtain a sufficiently fine power distribution, the pins were axially divided into 2 or 3 cm segments. The variations of the axial power profile between the segments are not higher than 1% in the central 30 cm section of each pin, or 5% in the 30 cm sections adjoining the central one. More details can be found in [14].
The neutron source emission spectrum was described using the ENDF/B-VII.1 prompt fission neutron spectrum. This approach is applicable because the emission spectra in the pins are nearly identical with the ^{235}U prompt fission neutron spectrum. Calculated relative uncertainties of the fluence rate in narrow 0.1 MeV energy groups are below 1-2% in the lower energy regions, and less than 10% in the high-energy regions. The uncertainties of the calculated reaction rates are lower than 1%, and the uncertainties in the fission densities are less than 0.5%.

4 Results

4.1 Power profile

The calculated power increase resulting from increased enrichment, shown in Fig. 2, was validated using measured fission densities. The comparison by means of C/E-1 agreement is

plotted in Fig. 3. It is worth noting that good agreement was reached in the selected positions in the boundary as well as in the central cut. Based on such agreement, it can be assumed that the perturbed neutron source used in the following calculations is reliable, and it indicates that the fission source uncertainty plays only a minor role in the total uncertainty of the neutron transport description in the RPV.

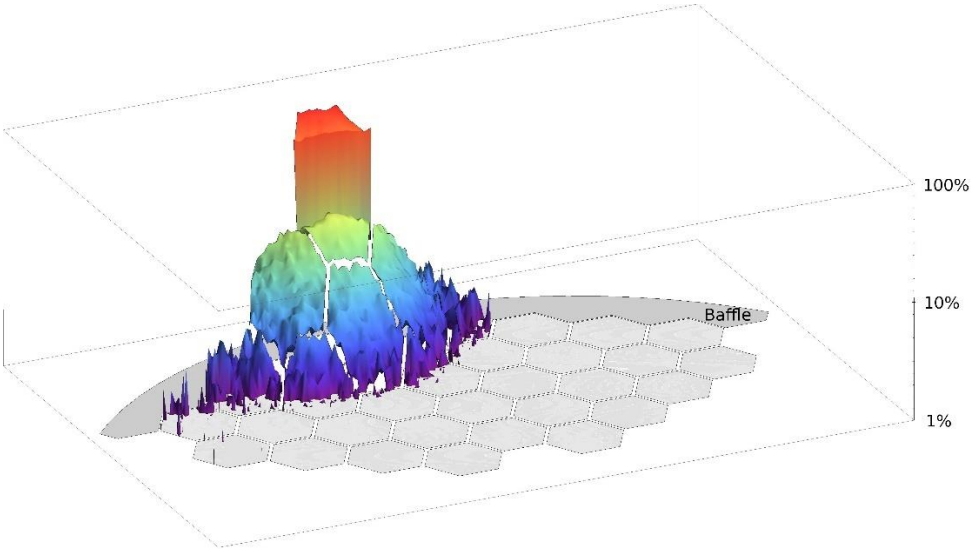

Fig. 2. Calculated power increase due to pin modification [11].

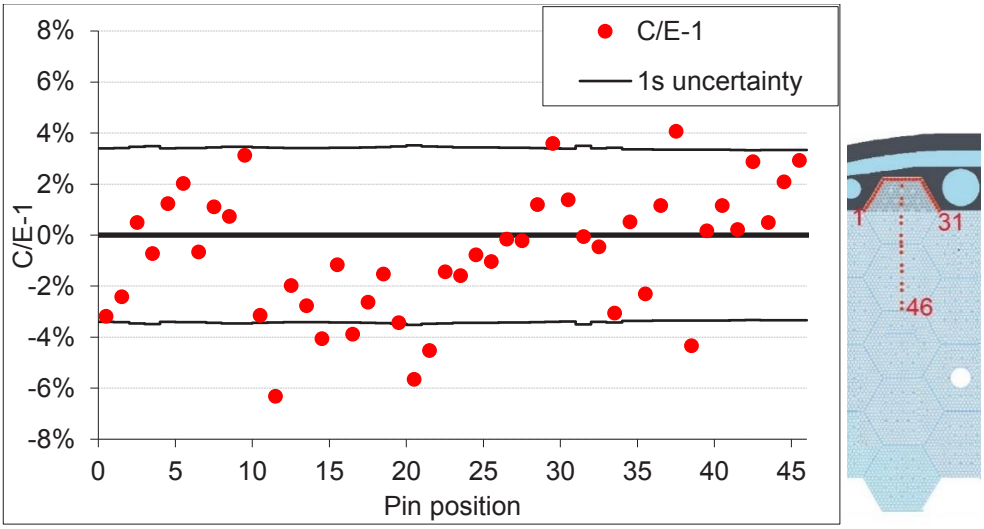

Fig. 3. C/E-1 for new source with increased local power with marked pins where validation was realised (left) and selection of pins on core layout (right).

4.2 Azimuthal profile behind the RPV simulator

The azimuthal profile of the neutron field behind the RPV was obtained by using the neutron fluxes above 1 MeV determined with a stilbene detector. This quantity is important for the determination of the local maxima in the neutron dose in the RPV, which is connected with the highest changes in the material properties of the RPV. Both the calculated and experimentally determined fluxes above 1 MeV in the azimuthal profile behind the RPV for the Mock-Up and perturbed case (when part of the boundary assembly contains higher enriched pins), normalised to average flux behind the RPV in each case, are plotted in Fig. 4. The indicated positions correspond to various angular positions with angular steps of 1.25 degrees between them. Generally, the calculated profile is smooth, while in the experimental profile several peaks occur. Although the shape of the calculated and experimental profile slightly differs, the variations are comparable with related uncertainties because the uncertainties in the azimuthal profile are about 5% (which covers uncertainty in the measured neutron fluxes and used scaling).

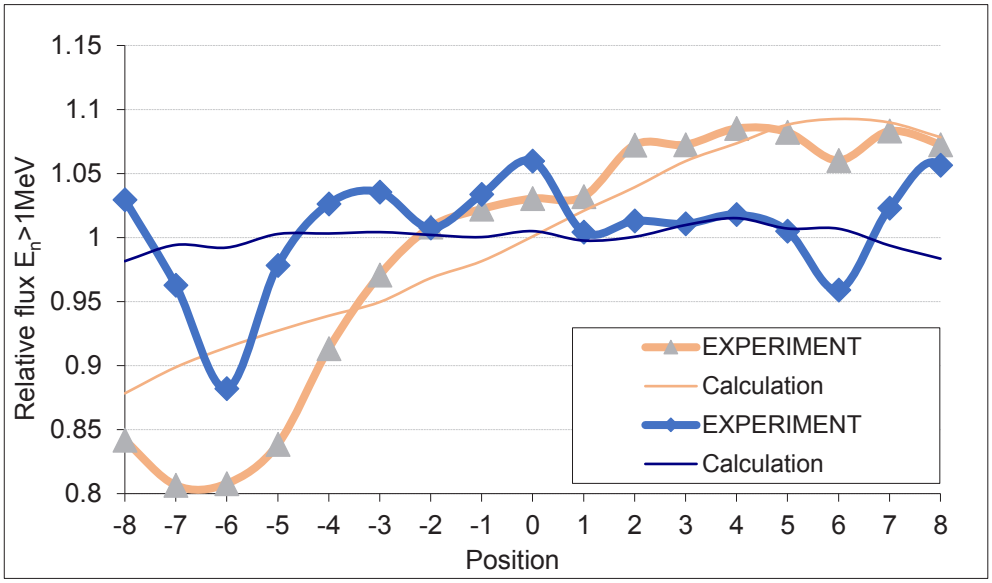

Fig. 4. Calculated and experimentally determined neutron flux profile in azimuthal direction with 1.25 degree steps for Mock-Up (blue) and perturbed (orange) case.

It can be seen in Fig. 4 that the power increase in the boundary assembly is reflected by a significant shift of the azimuthal profile behind the RPV. This result implies that a notable power shift in the core boundary is reflected by a local flux increase behind the RPV.
The direct increase in flux due to local power increase is plotted in Fig. 5. The graph indicates that in the more distant measuring points behind RPV the increase in flux is about 5%, in less distant points ~ 15%, and in positions closest to the replaced pins around 30%. The increase in the central position (denoted as “0”) is consistent with previous results where it was shown that the pins which were replaced contribute about 23% to the neutron flux behind the RPV [15], and the local power increase in the relevant pins is about 70%.

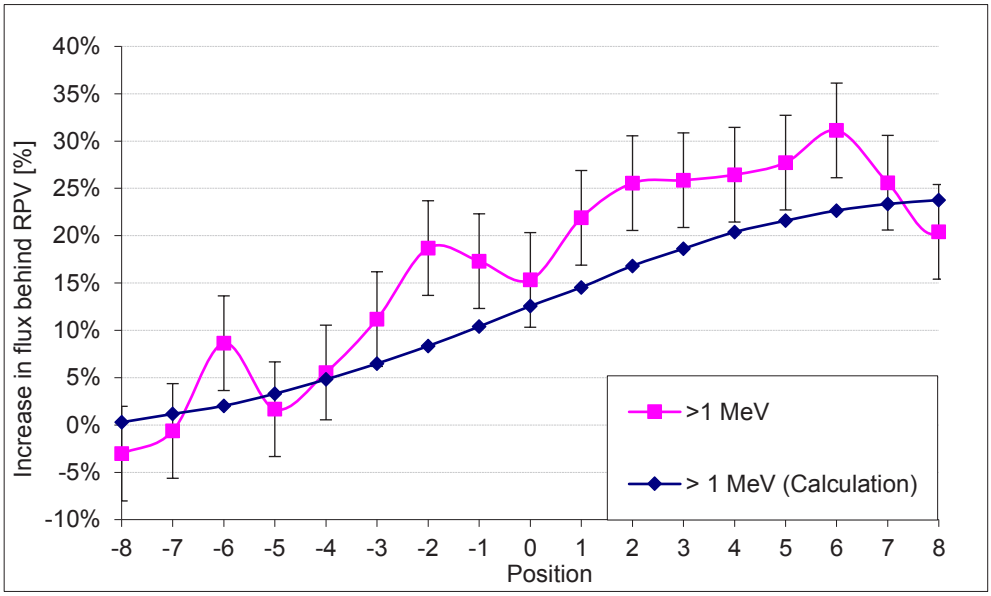

Fig. 5. Calculated and measured increase in the azimuthal profile of neutron flux E_n >1 MeV behind the RPV simulator when the 3.6% pins replaced the 2% enriched pins placed in the selected positions.

5 Conclusions

The realised experiments show a significant effect of the local power increase in the boundary region on the local flux increase in positions behind the RPV. These results are important, as the flux behind the RPV plays a crucial role in the evaluation of the residual lifetime. Due to rigorous characterisation of the neutron source, it is also possible to quantify the local flux increase based on the power increase. It can be concluded that this type of integral experiments, using a well-defined Mock-Up, can fill the gaps due to the lack of data from power reactors, where such measurements cannot be carried out. The spatial distribution of the neutron flux was measured using a stilbene detector covering the energy interval 0.9 – 10 MeV. The power density was characterised by gamma spectrometric measurements of fission products in selected irradiated fuel pins. The neutron flux in reactor internals was characterised using activation detectors.

The presented results were obtained using the CICRR infrastructure, which is financially supported by the Ministry of Education, Youth and Sports - project LM2023041 and by institutional support for the research organization development VAROPS awarded by the Ministry of Defence of the Czech Republic.

References

1. M. Kytka, M. Brumovský, Modification of WWER Standard Surveillance Programs for long term Operation and Annealing Mitigation Technical Meeting On Degradation Of Primary System Components Of Water Cooled Nuclear Power Plants: Current Issues And Future Challenges, (2013)

2. M. Marek, M. Brumovský,S. Vandlík, Spectral conditions in surveillance specimen container of Czech VVER-1000 reactors, Progress in Nuclear Science and Technology Volume 4 (2014) pp. 104-108
3. D. Harut, The influence of power distribution in core on radiation situation in reactor internals and pressure vessel of VVER-1000 reactor, PhD thesis
4. NRC 2001 Regulatory Guide 1.190, Calculational and dosimetry methods for determining pressure vessel neutron fluence, U.S. Nuclear Regulatory commission. March 2001
5. A.S.I., 2017 Association of Machinery Engineers normative Technical documentation about Evaluation of residual life equipment and pipes VVER nuclear power plants, Section IV, NTD A.S.I., (47), 2017
6. Schulc, M., Košťál, M., Czakoj, T. et al., Comprehensive stainless steel neutron transport libraries validation, Annals of Nuclear Energy, 2022, 179, 109433
7. M. Kostal, M. Švadlenková, J. Milčák, Absolute determination of power density in the VVER-1000 mock-up on the LR-0 research reactor, Appl. Rad. and Isot., Vol. 78, (2013), pp. 38-45
8. Zelong Zhao, Yaping Guo, Yisheng Zou et al., Validation and application of the Dragon5 lattice code for neutronics and burnup analysis of VVER-1000 pin cell and assembly model, Nucl. Eng. and Des., Vol. 407, (2023), 112279
9. M. Košťál, M. Schulc, V. Rypar, E. Novák, S. Zaritskyi, VVER-1000 Mock-up Physics Experiments Hexagonal Lattices (1.275 cm Pitch) of Low Enriched U(2.0, 3.0, 3.3 wt.% 235U)O2 Fuel Assemblies in Light Water with H3BO3, NEA/NSC/DOC(2006)1 LR(0)-VVER-RESR-002 CRIT RRATE POWDIS, benchmark OECD, NEA
10. M. Košťál, V. Rypar, E. Losa et al., The influence of core power distribution on neutron flux density behind a pressure vessel of a VVER-1000 Mock-Up in LR-0 reactor, Appl. Rad. and Isot., Vol. 142, (2018), pp 12–21
11. M. Košťál; E. Losa, M. Schulc et al., The effect of local power increase on radiation situation in internal parts of the VVER-1000 Mock-Up in LR-0 reactor, Ann. of Nucl. En., Vol. 121 (2018), pp. 567–576
12. T. Goorley, et al., "Initial MCNP6 Release Overview", Nuclear Technology, 180, pp 298-315 (Dec 2012)
13. M.B. Chadwick, M. Herman, P. Obložinský, et al, "ENDF/B-VII.1: Nuclear Data for Science and Technology: Cross Sections, Covariances, Fission Product Yields and Decay Data", Nucl. Data Sheets, 112, (2011), pp. 2887–2996
14. M. Košťál, F. Cvachovec, B. Jánský, V. Rypar, V. Juříček, D. Harutyunyan, M. Schulc, J. Milčák, E. Novák, S. Zaritsky, Neutron deep penetration through reactor pressure vessel and biological concrete shield of VVER-1000 Mock-Up in LR-0 reactor, Ann. of Nucl. En., Vol. 94, (2016), pp. 672-683
15. M. Košťál, VVER-1000 Neutronics, Transport of Neutrons and Photons in Construction Parts of VVER 1000 Reactor, 978-3-8484-8658-8